

# Monitoring statistics of the ERS-2 scatterometer for ESA cycle 109

(Project Ref. 18212/04/I-OL)

Hans Hersbach

European Centre for Medium-Range Weather Forecasts,

Shinfield Park, Reading, RG2 9AX, England

Tel: (+44 118) 9499476, e-mail: dal@ecmwf.int

October 28, 2005

## 1 Introduction

The quality of the UWI product was monitored at ECMWF for cycle 109. Results were compared to those obtained from the previous cycle, as well for data received during the nominal period in 2000 (up to cycle 59). No corrections for duplicate observations were applied.

During cycle 109 data was received between 21:04 UTC 19 September 2005 and 20:57 UTC 24 October 2005. No data was received for the 6-hourly batch centred around 00 UTC 11 October 2005.

Data is being recorded whenever within the visibility range of a ground station. For cycle 109 data coverage was over the North-Atlantic, part of the Mediterranean, the Caribbean, the Gulf of Mexico, a small part of the Pacific west from the US Canada and Central America, the Chinese and Japanese Sea, and the Southern Ocean south of Australia and New Zealand (see Figure 2).

During the last two weeks of cycle 109, the asymmetry between the fore and aft incidence angles showed less volatile peaks than for previous cycles. Especially from 16 October 2005 onwards, fluctuations were so small that the  $k_p$ -yaw ESA flag was hardly activated. Solar activity was low (source:www.spaceweather.com).

Compared to cycle 108, the UWI wind speed relative to ECMWF first-guess (FG) fields showed an increased standard deviation (from 1.42 to 1.50 m/s), representing a natural seasonal trend, also observed one year ago. Bias levels have become less negative (from -0.95 m/s to -0.82 m/s), the same pattern being observed for QuikSCAT data within the area of ERS-2 data coverage.

Between 4 October and 20 October 2005 the performance of the UWI wind direction was slightly degraded. CMOD4 winds that were de-aliased with ECMWF FG winds did not show such a behaviour, which indicates temporary de-aliasing problems of the UWI product. For the remainder of cycle 109, the performance of the UWI wind direction was nominal.

Ocean calibration shows that inter-node and inter-beam dependency of bias levels were further reduced. The overall negative bias level diminished as well (-0.50 dB, was -0.71 dB, see Figure 4).

The ECMWF assimilation/forecast system was not changed during cycle 109.

The cycle-averaged evolution of performance relative to ECMWF first-guess (FG) winds is displayed in Figure 1. Figure 2 shows global maps of the over cycle 109 averaged UWI data coverage and wind climate, Figure 3 for performance relative to FG winds.

## **2 ERS-2 statistics from 19 September to 24 October 2005**

### **2.1 Sigma0 bias levels**

The average sigma0 bias levels (compared to simulated sigma0's based on ECMWF model FG winds) stratified with respect to antenna beam, ascending or descending track and as function of incidence angle (i.e. across-node number) is displayed in Figure 4.

Inter-node and inter-beam (mainly mid versus the fore/aft beam) dependencies are smaller than for cycles 108. However, at high range, backscatter from the mid antenna is still about 0.2 dB higher than that for the other two antennas. Average bias level is less negative (-0.50 dB, was -0.71 dB), now being less negative to that for nominal data in 2000 (see Figure 1 of the reports for cycle 48 to 59).

The data volume of descending tracks was about 8% lower than for ascending tracks.

### **2.2 Incidence angles**

For ESACA, across-node binning is, like the old processor, retained on a 25km mesh. From simple geometrical arguments it follows that variations in yaw attitude will lead to asymmetries between the incidence angles of the fore and aft beam. Indeed, this has been observed. Figure 5 gives a time evolution of this asymmetry, showing rapid variations, which are typical for yaw attitude errors. Also in this Figure, the occasions for which the combined  $k_p$ -yaw quality flag was set are indicated by red stars. The relation with incidence-angle asymmetries is obvious.

For cycle 109, there were only a few large peaks, e.g., for 23 September and 8 October 2005. During the last two weeks of cycle 109, fluctuations calmed down, especially from 12 October 2005 onwards. As a result, the  $k_p$ -yaw quality was hardly active, resulting in much larger quantities of data passing quality control (QC). Solar

activity was low during cycle 109.

### 2.3 Distance to cone history

The distance to the cone history is shown in Figure 6. Curves are based on data that passed all QC, including the test on the  $k_p$ -yaw flag, and subject to the land and sea-ice check at ECMWF (see cyclic report 88 for details).

Like for cycle 108, time series are (due to lack of statistics) very noisy, especially for the near-range nodes. Most spikes were found to be the result of low data volumes.

Compared to cycle 108, the average level was unaltered (1.17), i.e., about 7% higher than for nominal data (see top panel Figure 1).

The fraction of data that did not pass QC is displayed in Figure 6 as well (dash curves). Note that, thanks to the lower activity of the  $k_p$ -yaw flag, more data was accepted from 12 October 2005 onwards.

### 2.4 UWI minus First-Guess wind history

In Figure 7, the UWI minus ECMWF first-guess wind-speed history is plotted.

The history plot shows several peaks, most of which are related to low data volumes. Similar results apply for the history of de-aliased CMOD4 winds versus FG (Figure 9).

Figure 11 displays the locations for which UWI winds were more than 8 m/s weaker (top panel) and more than 8 m/s stronger (lower panel) than FG winds. Like for cycle 108, such collocations are isolated, and usually indicate meteorologically active regions, for which UWI data and ECMWF model field show reasonably small differences in phase and/or intensity.

Two cases are presented in Figure 12. The top panel shows the capture of Typhoon Saola on 29 September 2005 (Category 2). Although both de-aliased CMOD5 (rather than UWI) and ECMWF FG winds agree well in position, CMOD5 winds are, especially near the cyclone centre, much stronger (up to 32 m/s versus 18 m/s). The scatterometer winds show in addition a more asymmetric structure. The lower panel shows Hurricane Wilma, observed on 29 October 2005 (Category 3 at that time), 8 hours before it made landfall at the southern part of Florida. Also here, CMOD5 winds are stronger near the centre of the hurricane (up to 29.5 m/s versus 23.3 m/s for ECMWF). In addition, there is a small shift in position. Both the scatterometer data for Saola and Wilma were actively assimilated, although due to too large differences in wind speed, winds near the centre of Saola were rejected.

Average bias levels and standard deviations of UWI winds relative to FG winds are displayed in Table 1. From this it is seen that the bias of both the UWI and CMOD4 product have become less negative, and are now comparable to that for nominal data in 2000 (UWI: -0.82 m/s now, was -0.79 m/s for cycle 59).

The trend of a large increase of negative bias between April and July, followed by a swift recovery starting in July was also observed in 2004. As was highlighted in the previous cyclic reports, it is now believed that this yearly trend is induced by chang-

	cycle 108		cycle 109	
	UWI	CMOD4	UWI	CMOD4
speed STDV	1.42	1.41	1.50	1.49
node 1-2	1.47	1.46	1.61	1.57
node 3-4	1.41	1.40	1.53	1.51
node 5-7	1.38	1.38	1.46	1.46
node 8-10	1.36	1.36	1.42	1.43
node 11-14	1.38	1.38	1.45	1.45
node 15-19	1.41	1.40	1.47	1.47
speed BIAS	-0.95	-0.95	-0.82	0.81
node 1-2	-1.41	-1.39	-1.35	-1.31
node 3-4	-1.20	-1.16	-1.11	-1.05
node 5-7	-1.00	-0.96	-0.88	-0.84
node 8-10	-0.83	-0.82	-0.68	-0.67
node 11-14	-0.76	-0.77	-0.62	-0.63
node 15-19	-0.79	-0.81	-0.61	-0.63
direction STDV	41.0	19.1	30.4	19.5
direction BIAS	-1.7	-3.0	-3.1	-3.0

Table 1: Biases and standard deviation of ERS-2 versus ECMWF FG winds in m/s for speed and degrees for direction.

ing local geophysical conditions, variation in the atmospheric density stratification being the most likely candidate. Strong indication for this is a similar trend observed for QuikSCAT data when restricted to an area well-covered by ERS-2 (20N-90N, 80W-20E). In Figure 17 time series are shown for that area for both ERS-2 (top panel) and QuikSCAT (lower panel) for the period between 1 January 2004 and 24 October 2005 (end of cycle 109). Results are displayed for at ECMWF actively assimilated data, i.e., CMOD5 winds for ERS-2 and 4%-reduced QuikSCAT winds on a 50km resolution. It shows a rapid increase of scatterometer winds relative to model winds since half of July 2005, confirming the observed decreased negative bias for the UWI product.

The standard deviation of UWI wind speed compared to cycle 108 has increased (1.50 m/s, was 1.42 m/s), the main reason being a less mild wind climate.

For cycle 109 the (UWI - FG) direction standard deviations were mostly ranging between 20 and 40 degrees (Figure 8). However, between 4 October and 20 October 2005, performance of the UWI wind direction was slightly degraded. For these periods, at ECMWF de-aliased CMOD4-based winds did not show peaks, therefore, indicating temporary problems with the de-aliasing of the UWI product.

Compared to cycle 108 (that contained three anomalies periods) the average performance for UWI wind direction has improved (STDV 30.4 degrees, was 41.1 degrees), while that of de-aliased CMOD4 winds was more stable (STDV 19.5 degrees, was 19.1 degrees).

## 2.5 Scatterplots

Scatterplots of FG winds versus ERS-2 winds are displayed in Figures 13 to 16. Values of standard deviations and biases are slightly different from those displayed in Table 1. Reason for this is that, for plotting purposes, the in 0.5 m/s resolution ERS-2 winds have been slightly perturbed (increases scatter with 0.02 m/s), and that zero wind-speed ERS-2 winds have been excluded (decreases scatter by about 0.05 m/s).

The scatterplot of UWI wind speed versus FG (Figure 13) is very similar to that for (at ECMWF inverted) de-aliased CMOD4 winds (Figure 15). It confirms that the ESACA inversion scheme is working properly.

Winds derived on the basis of CMOD5 are displayed in Figure 16. The relative standard deviation is lower than for CMOD4 winds (1.49 m/s versus 1.52 m/s). Compared to ECMWF FG, CMOD5 winds are 0.29 m/s slower; this average arising from mostly moderate winds. However, also for the more extreme winds there is a tendency of underestimation.

## Figure Captions

**Figure 1:** Evolution of the performance of the ERS-2 scatterometer averaged over 5-weekly cycles from 12 December 2001 (cycle 69) to 24 October 2005 (end cycle 109) for the UWI product (solid, star) and de-aliased winds based on CMOD4 (dashed, diamond). Results are based on data that passed the UWI QC flags. For cycle 85 two values are plotted; the first value for a global set, the second one for a regional set (for details see the corresponding cyclic report). Dotted lines represent values for cycle 59 (5 December 2000 to 17 January 2001), i.e. the last stable cycle of the nominal period. From top to bottom panel are shown the normalized distance to the cone (CMOD4 only) the standard deviation of the wind speed compared to FG winds, the corresponding bias (for UWI winds the extremes in node-wise averages are shown as well), and the standard deviation of wind direction compared to FG.

**Figure 2:** Average number of observations per 12H and per 125km grid box (top panel) and wind-climate (lower panel) for UWI winds that passed the UWI flags QC and a check on the collocated ECMWF land and sea-ice mask.

**Figure 3:** The same as Figure 2, but now for the relative bias (top panel) and standard deviation (lower panel) with ECMWF first-guess winds.

**Figure 4:** Ratio of  $< \sigma_0^{0.625} > / < \text{CMOD4}(\text{FirstGuess})^{0.625} >$  converted in dB for the fore beam (solid line), mid beam (dashed line) and aft beam (dotted line), as a function of incidence angle for descending and ascending tracks. The thin lines indicate the error bars on the estimated mean. First-guess winds are based on the in time closest (+3h, +6h, +9h, or +12h) T511 forecast field, and are bilinearly interpolated in space.

**Figure 5:** Time series of the difference in incidence angle between the fore and aft beam. Red stars indicate the occurrences for which the combined  $k_p$ -yaw flag was set.

**Figure 6:** Mean normalized distance to the cone computed every 6 hours for nodes 1-2, 3-4, 5-7, 8-10, 11-14 and 15-19). The dotted curve shows the number of incoming triplets in logarithmic scale (1 corresponds to 60,000 triplets) and the dashed one indicates the fraction of complete (based on the land and sea-ice mask at ECMWF) sea-located triplets rejected by ESA flags, or by the wind inversion algorithm (0: all data kept, 1: no data kept).

**Figure 7:** Mean (solid line) and standard deviation (dashed line) of the wind speed difference UWI - first guess for the data retained by the quality control.

**Figure 8:** Same as Fig. 7, but for the wind direction difference. Statistics are computed for winds stronger than 4 m/s.

**Figures 9 and 10:** Same as Fig. 7 and 8 respectively, but for the de-aliased CMOD4 data.

**Figure 11:** Locations of data during cycle 109 for which UWI winds are more than 8 m/s weaker (top panel) respectively stronger (lower panel) than FG, and on which QC on UWI flags and the ECMWF land/sea-ice mask was applied.

**Figure 12:** Comparison between de-aliased CMOD5 (red) and ECMWF FG (blue) winds for Typhoon Saola on 24 September 2005 (top panel) and Hurricane Wilma on 24 October 2005 (lower panel).

**Figure 13:** Two-dimensional histogram of first guess and UWI wind speeds, for the data kept by the UWI flags, and QC based on the ECMWF land and sea-ice mask. Circles denote the mean values in the y-direction, and squares those in the x-direction.

**Figure 14:** Same as Fig. 13, but for wind direction. Only winds stronger than 4m/s are taken into account.

**Figure 15:** Same as Fig. 13, but for de-aliased CMOD4 winds.

**Figure 16:** Same as Fig. 13, but for de-aliased CMOD5 winds.

**Figure 17:** Wind-speed bias relative to FG winds for actively assimilated ERS-2 winds (based on CMOD5) for nodes 1-19 (top panel) respectively 50-km QuikSCAT (based on the QSCAT-1 model function and reduced by 4%) for nodes 5-34 (lower panel), averaged over the area (20N-90N, 80W-20E), and displayed for the period 01 January 2004 - 24 October 2005. Curves represent centred 15-day running means. Vertical dashed blue lines mark ECMWF model changes.

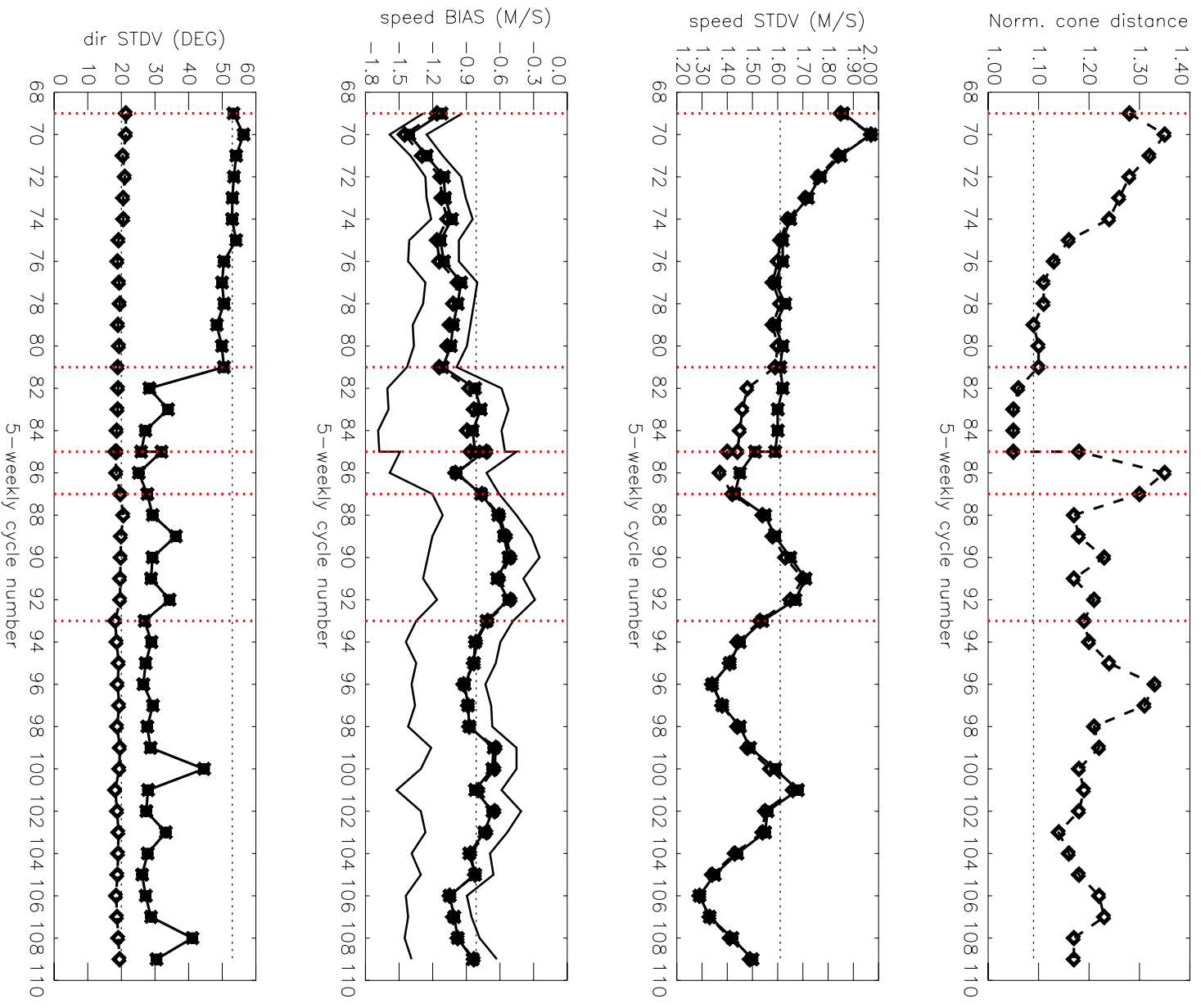
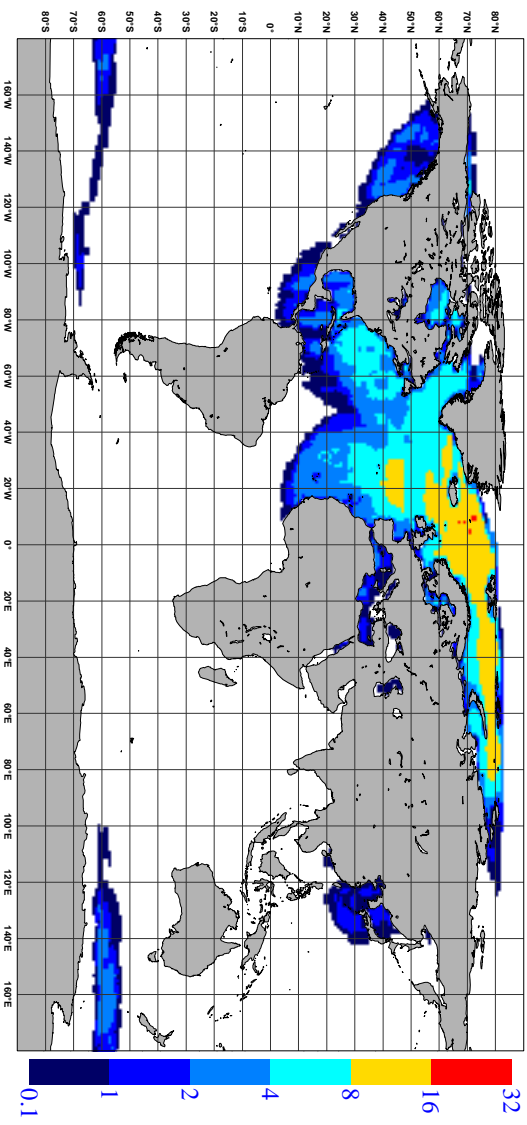


Figure 1

NOBS ( ERS-2 UWI ), per 12H, per 125km box  
average from 2005092000 to 2005102418 GLOB:3.06



AVERAGE ( ERS-2 UWI ), in m/s.  
average from 2005092000 to 2005102418 GLOB:6.78

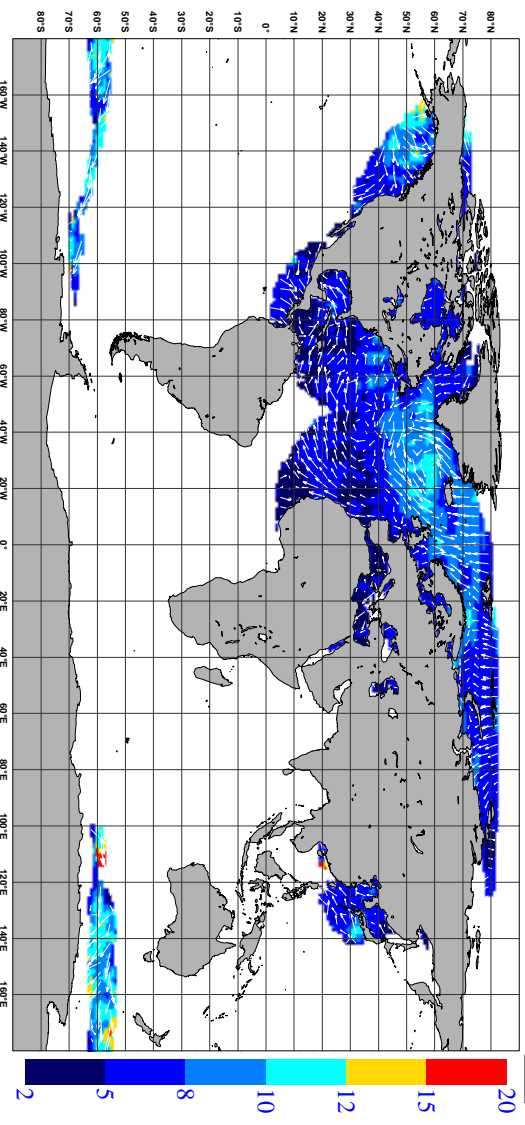
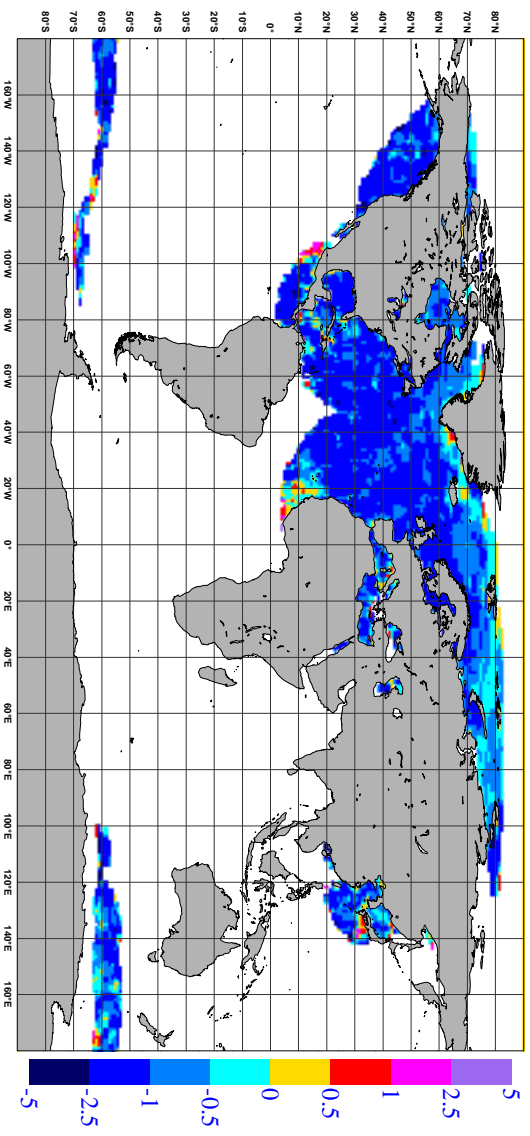


Figure 2



BIAS ( ERS-2 UWI vs FIRST-GUESS ), in m/s.  
average from 2005092000 to 2005102418 GLOB:-1.06



STDV ( ERS-2 UWI vs FIRST-GUESS ), in m/s.  
average from 2005092000 to 2005102418 GLOB:1.2

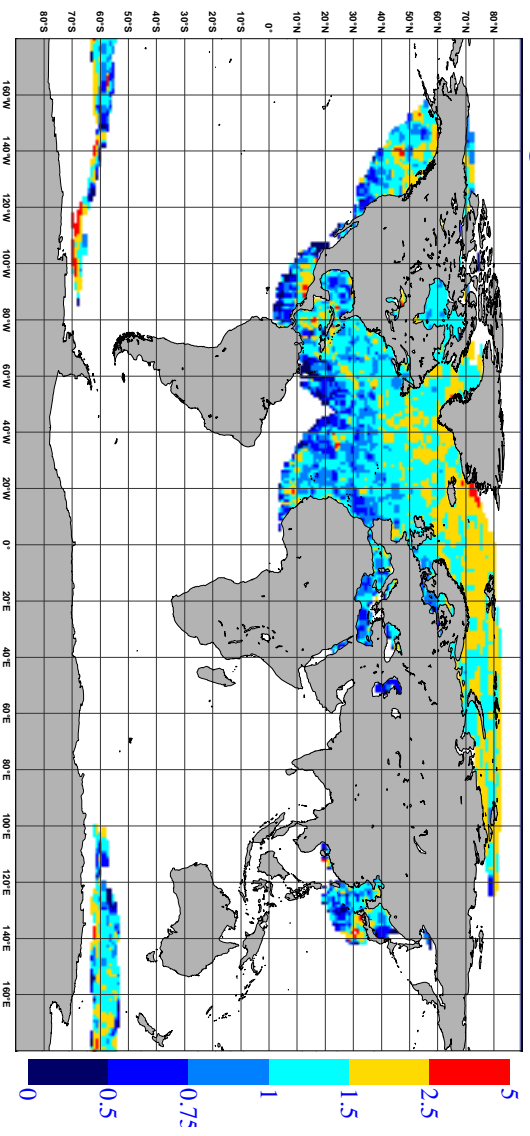


Figure 3

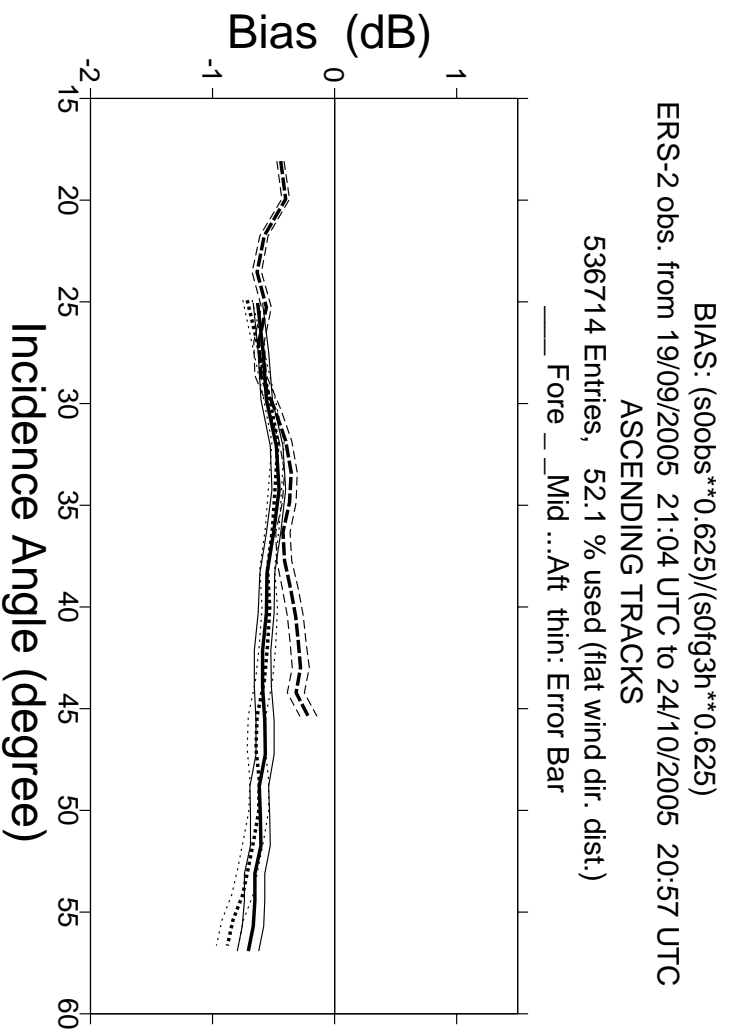
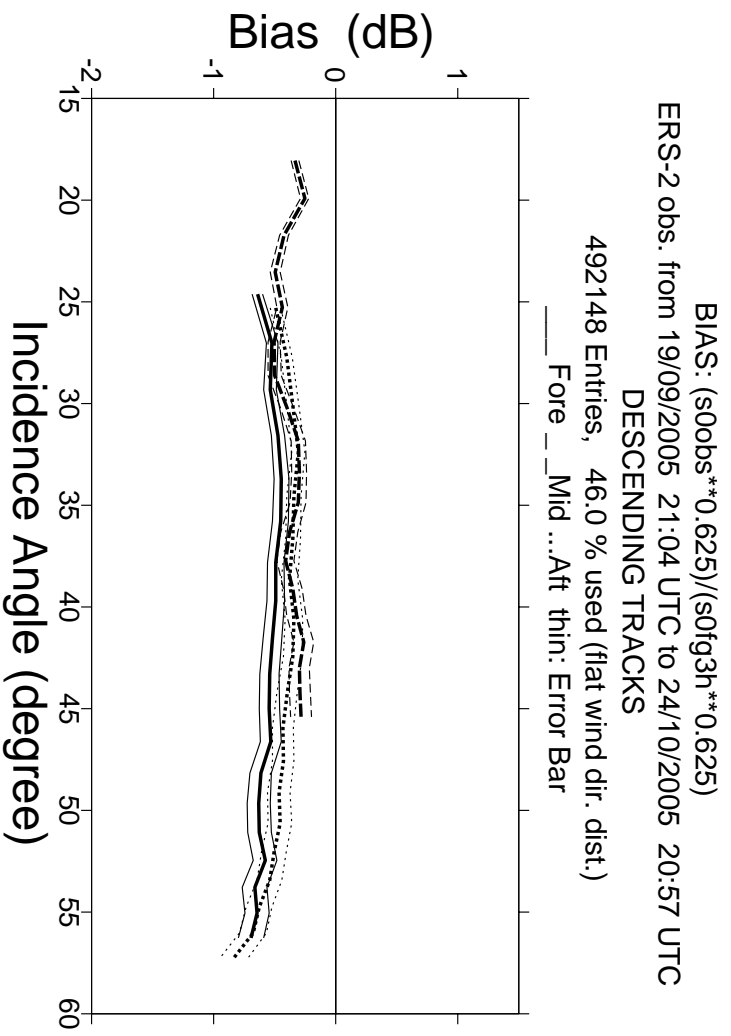


Figure 4

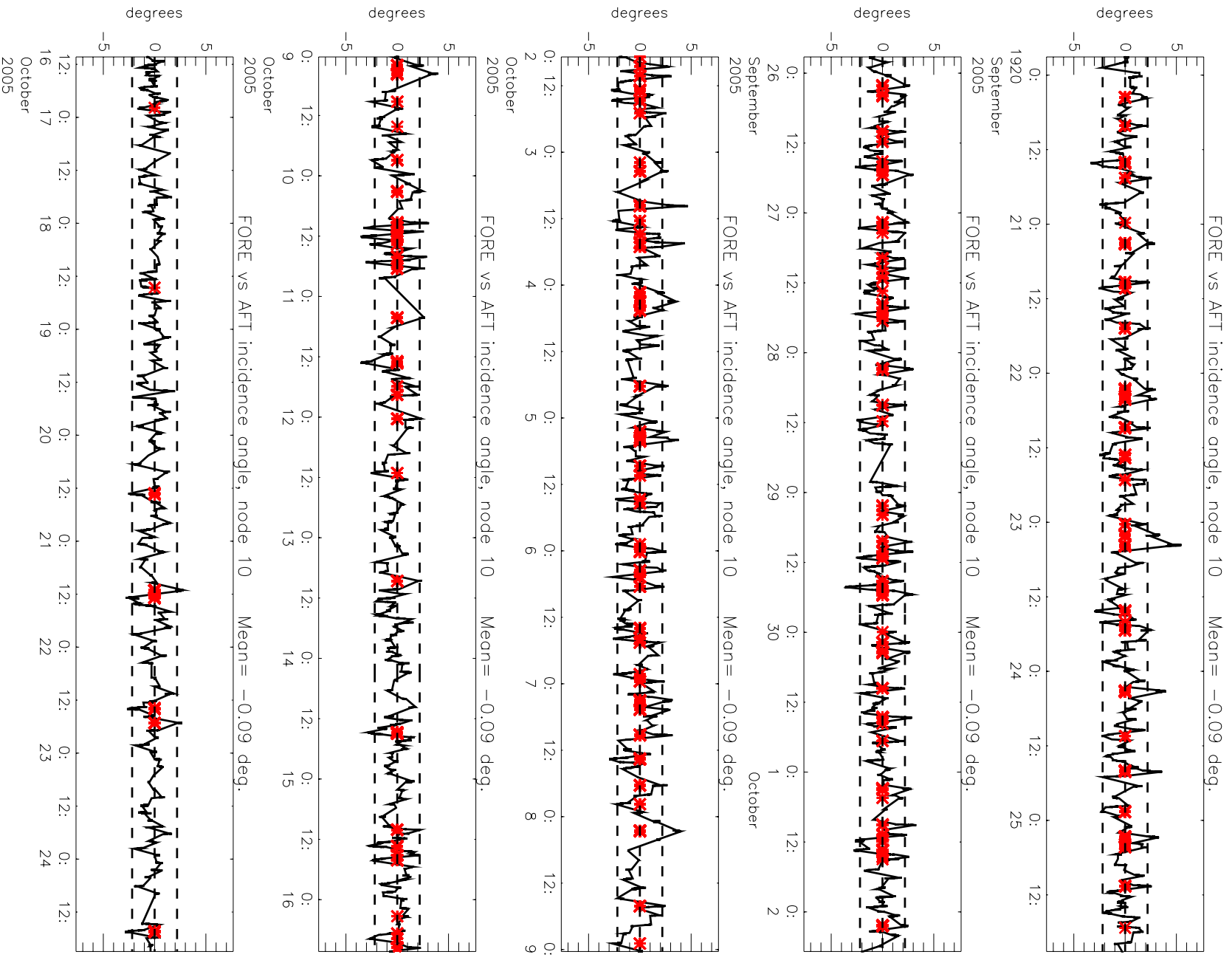


Figure 5

# Monitoring of Sigma0 triplets versus CMOD4 for ERS-2

from 2005092000 to 2005102418

(solid) mean normalised distance to the cone over 6 h

(dashed) fraction of complete sea-point observations rejected by ESA flag or CMOD4 inversion

(dotted) total number of data in log. scale (1 for 60000)

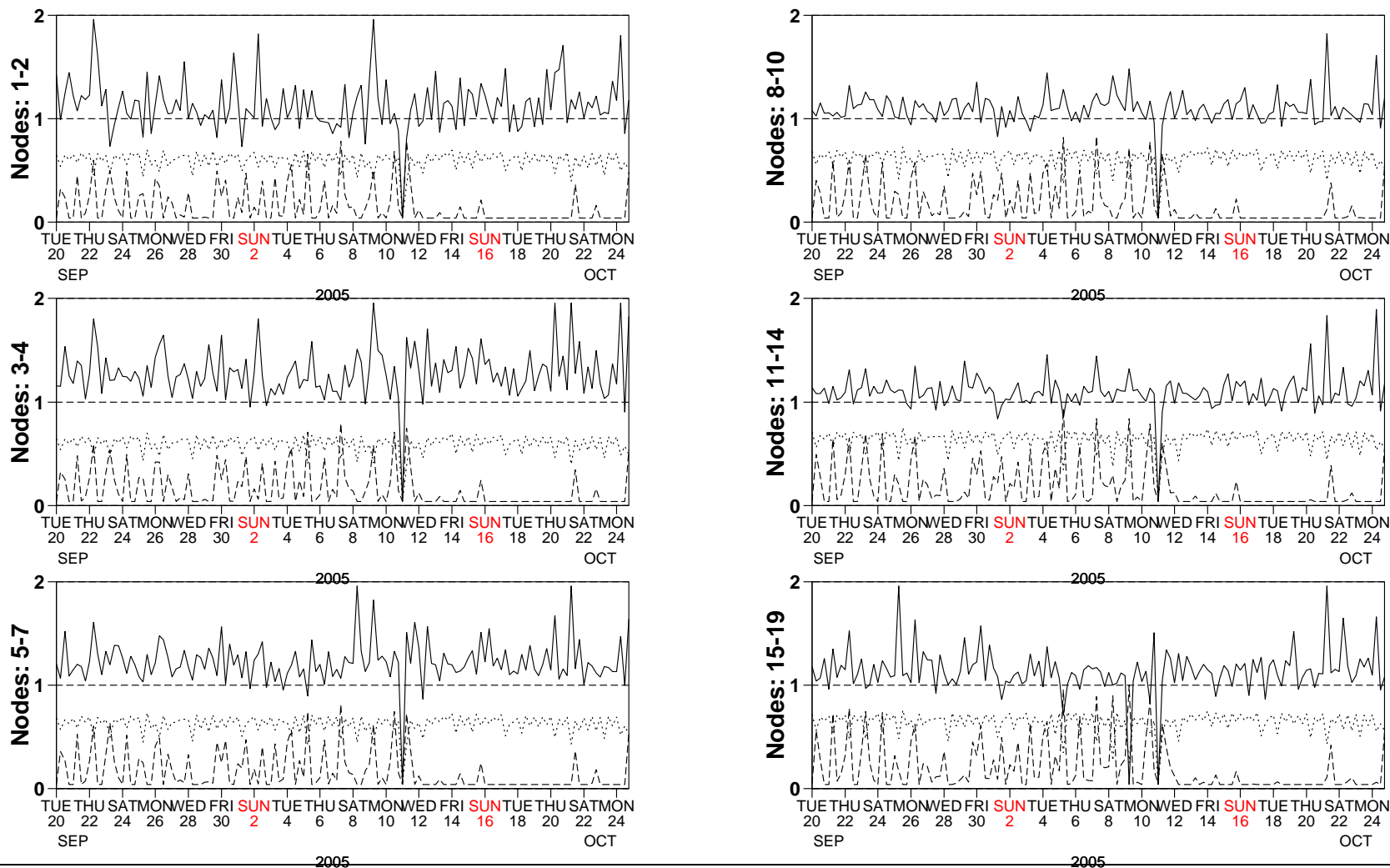


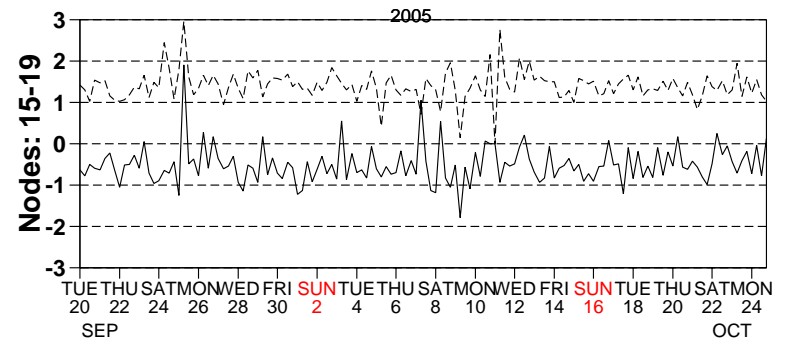
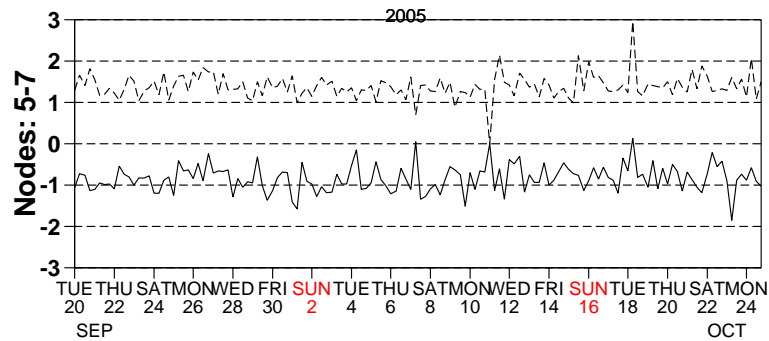
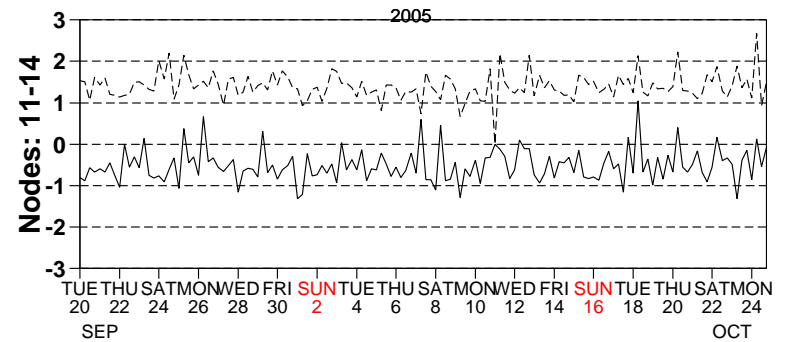
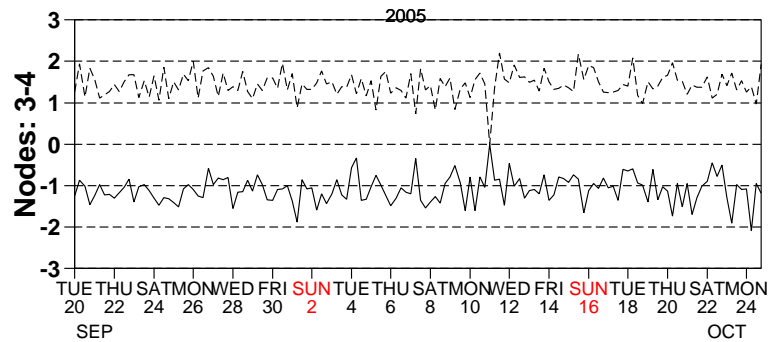
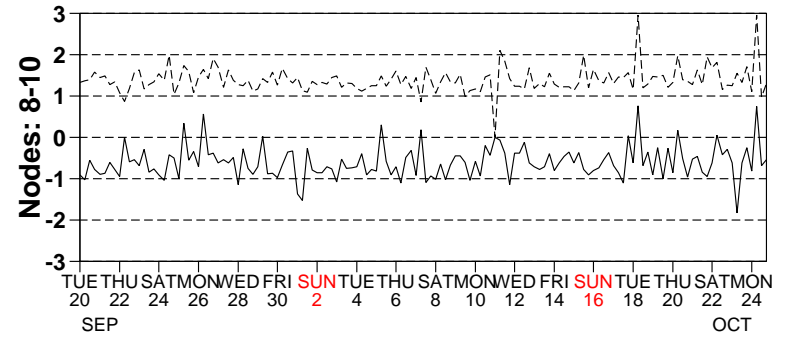
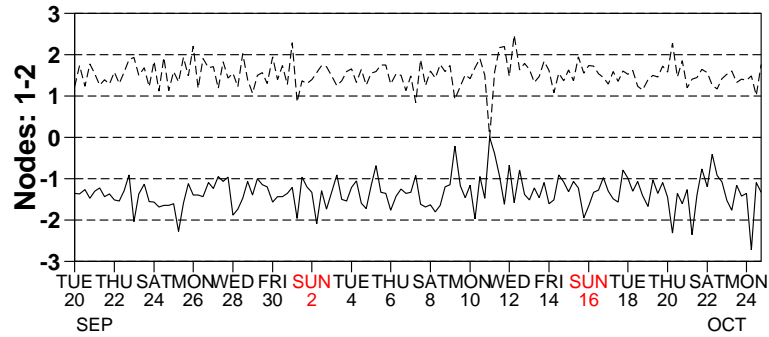
Figure 6

# Monitoring of UWI winds versus First Guess for ERS-2

from 2005092000 to 2005102418

(solid) wind speed bias UWI - First Guess over 6h (deg.)

(dashed) wind speed standard deviation UWI - First Guess over 6h (deg.)



2005

2005

Figure 7

# Monitoring of UWI winds versus First Guess for ERS-2

from 2005092000 to 2005102418

(solid) wind direction bias UWI - First Guess over 6h (deg.)

(dashed) wind direction standard deviation UWI - First Guess over 6h (deg.)

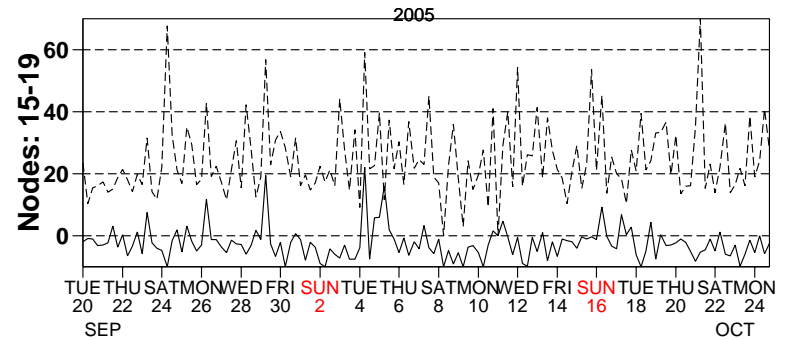
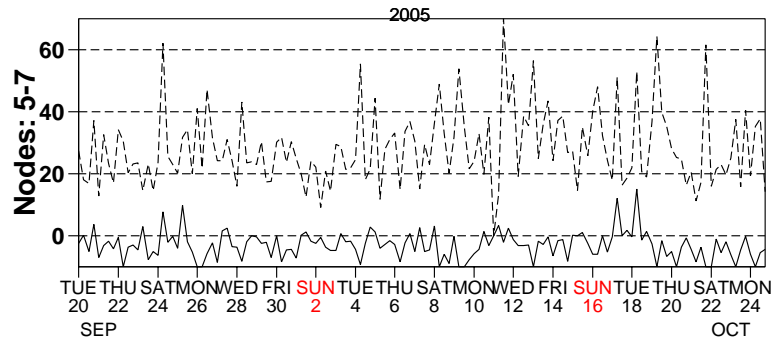
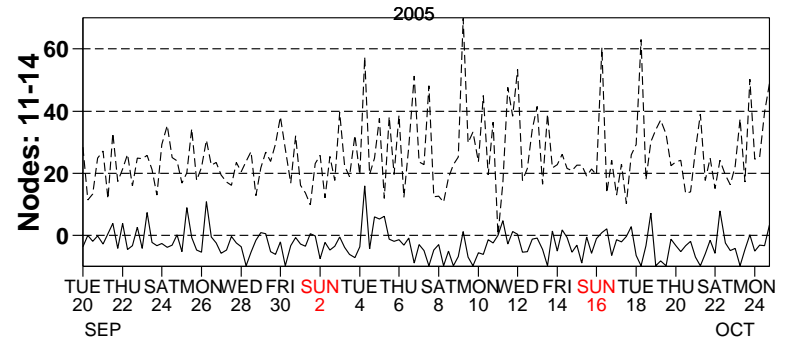
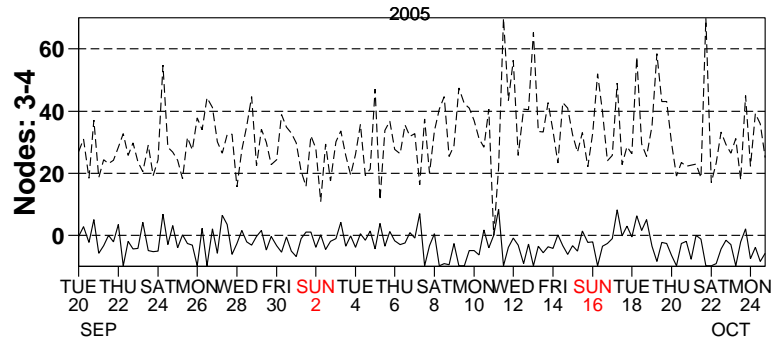
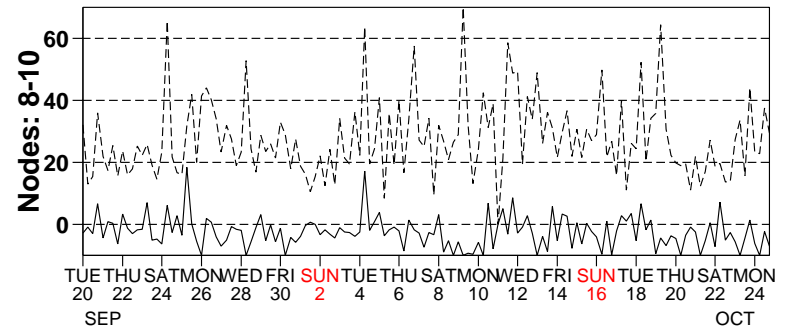
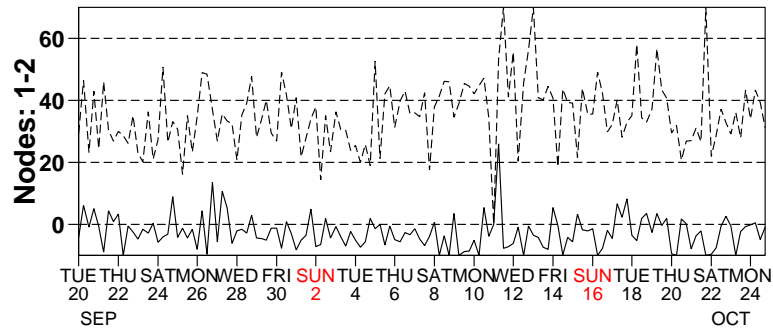


Figure 8

# Monitoring of de-aliased CMOD4 winds versus First Guess for ERS-2

from 2005092000 to 2005102418

(solid) wind speed bias CMOD4 - First Guess over 6h (deg.)

(dashed) wind speed standard deviation CMOD4 - First Guess over 6h (deg.)

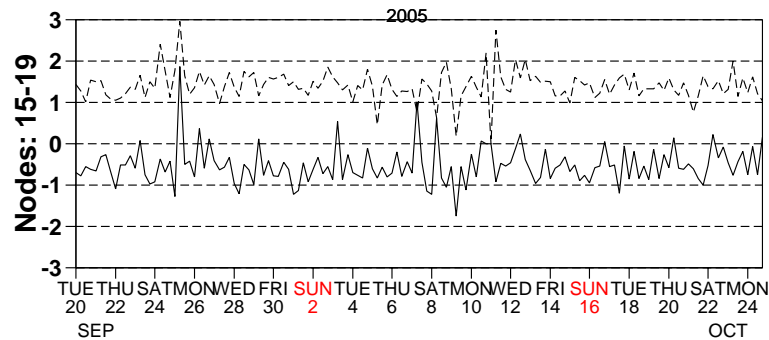
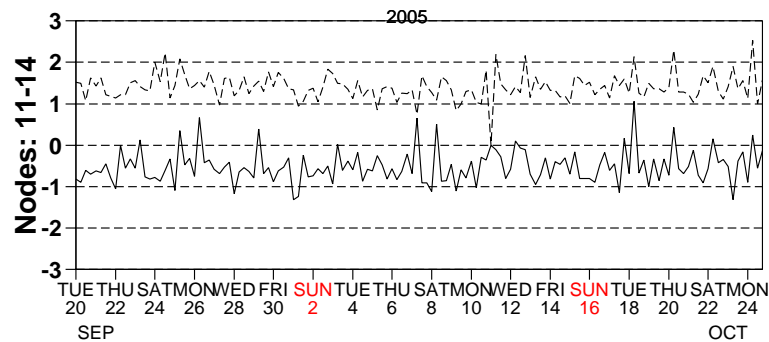
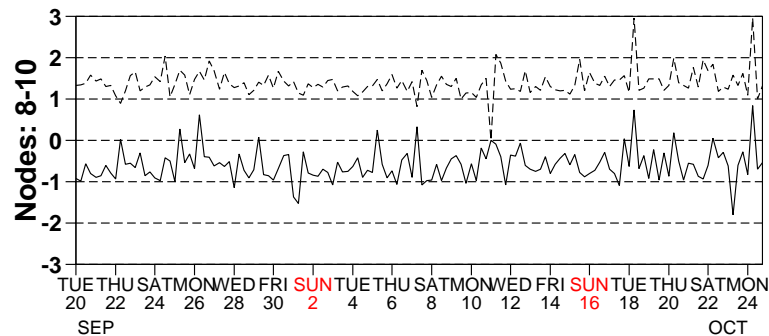
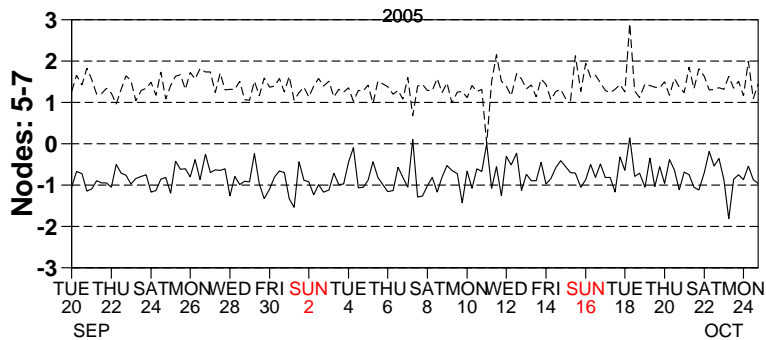
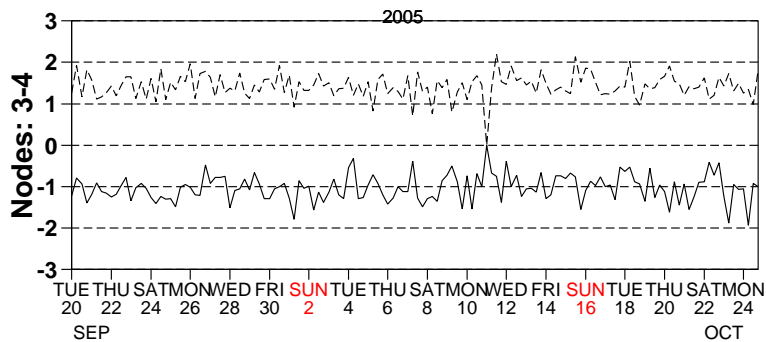
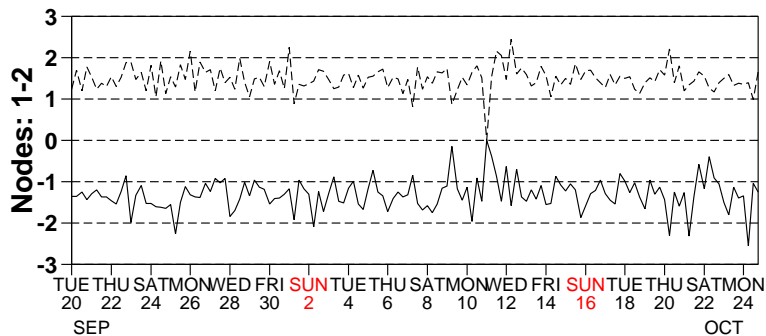


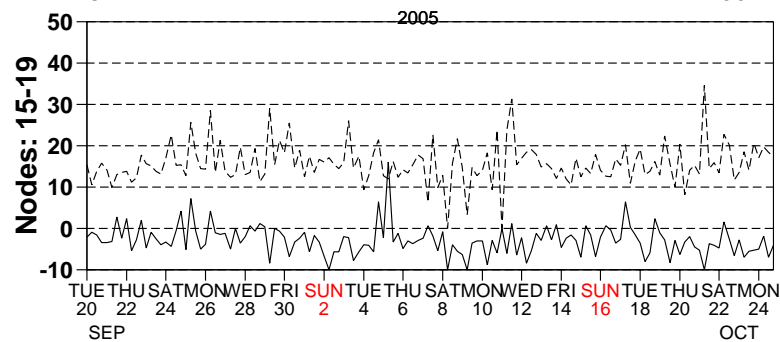
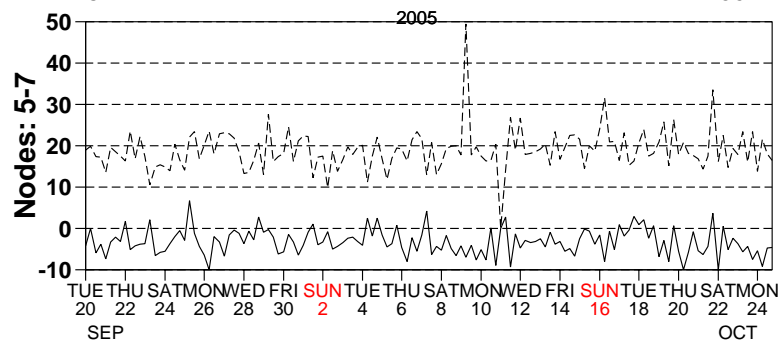
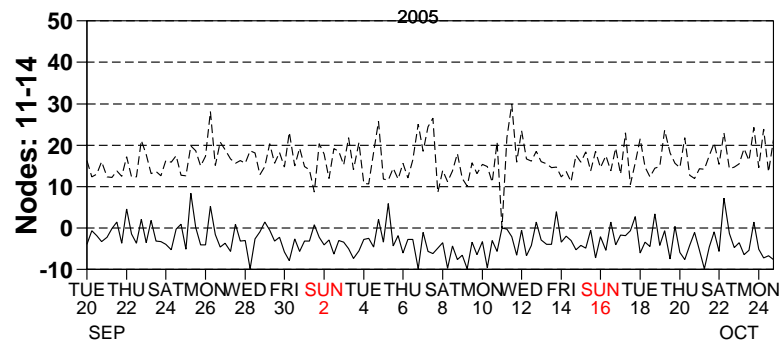
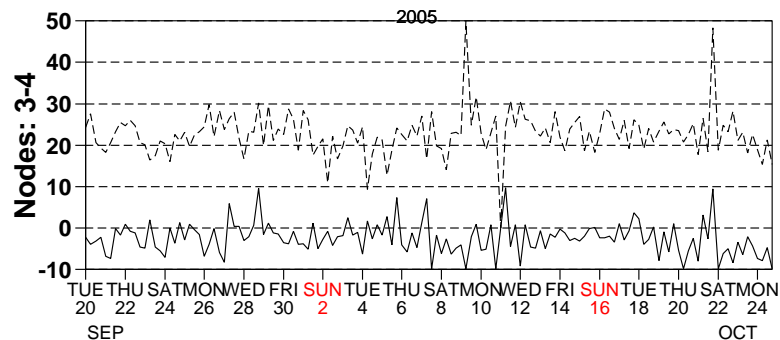
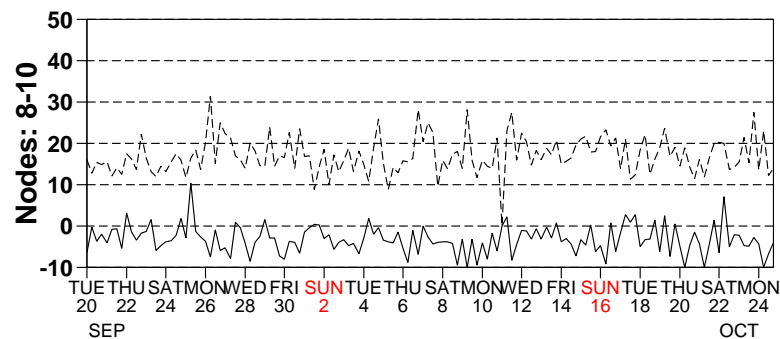
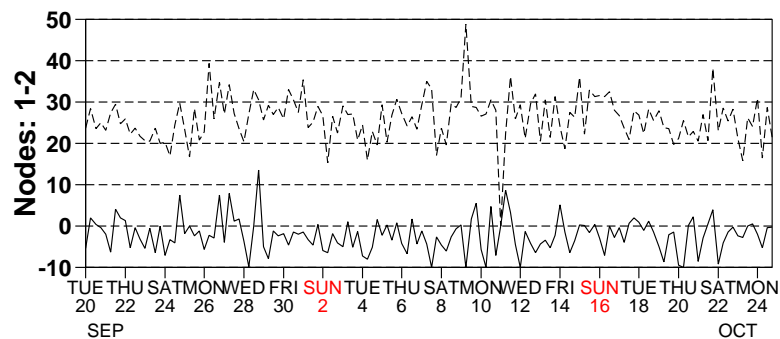
Figure 9

# Monitoring of de-aliased CMOD4 winds versus First Guess for ERS-2

from 2005092000 to 2005102418

(solid) wind direction bias CMOD4 - First Guess over 6h (deg.)

(dashed) wind direction standard deviation CMOD4 - First Guess over 6h (deg.)



2005

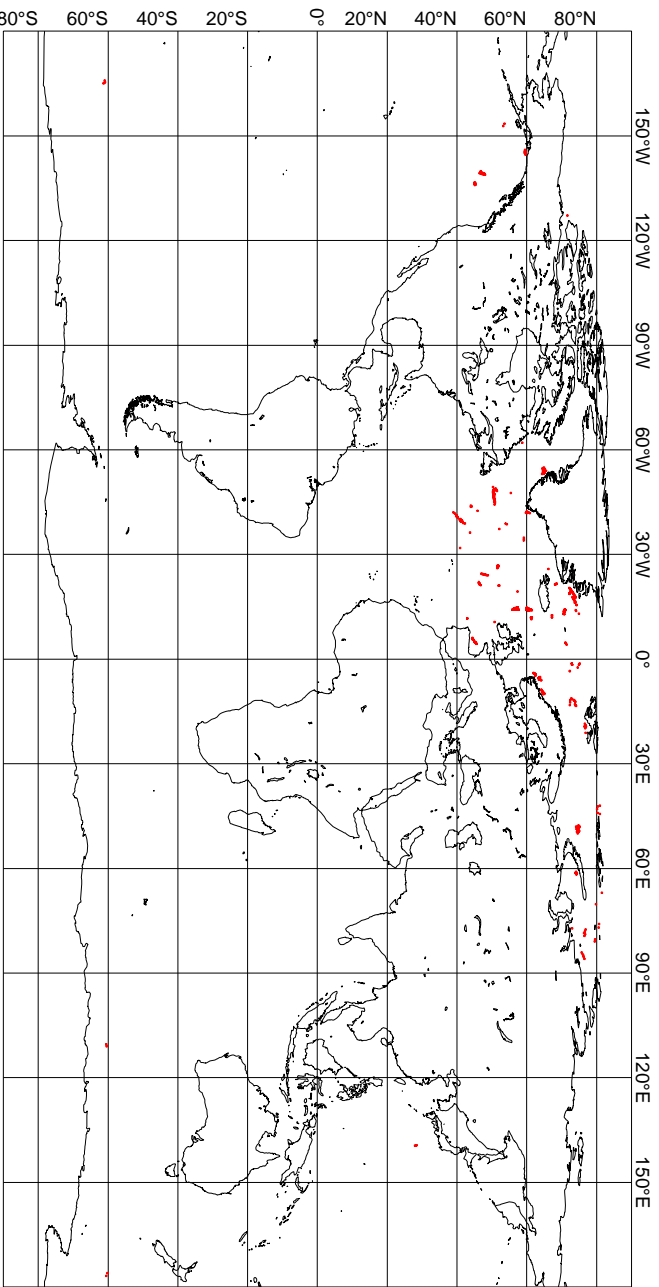
2005

Figure 10



UWI winds more than 8 m/s weaker than FGAT

CYCLE 109, 2005092000 to 2005102418, QC on ESA flags



UWI winds more than 8 m/s stronger than FGAT

CYCLE 109, 2005092000 to 2005102418, QC on ESA flags

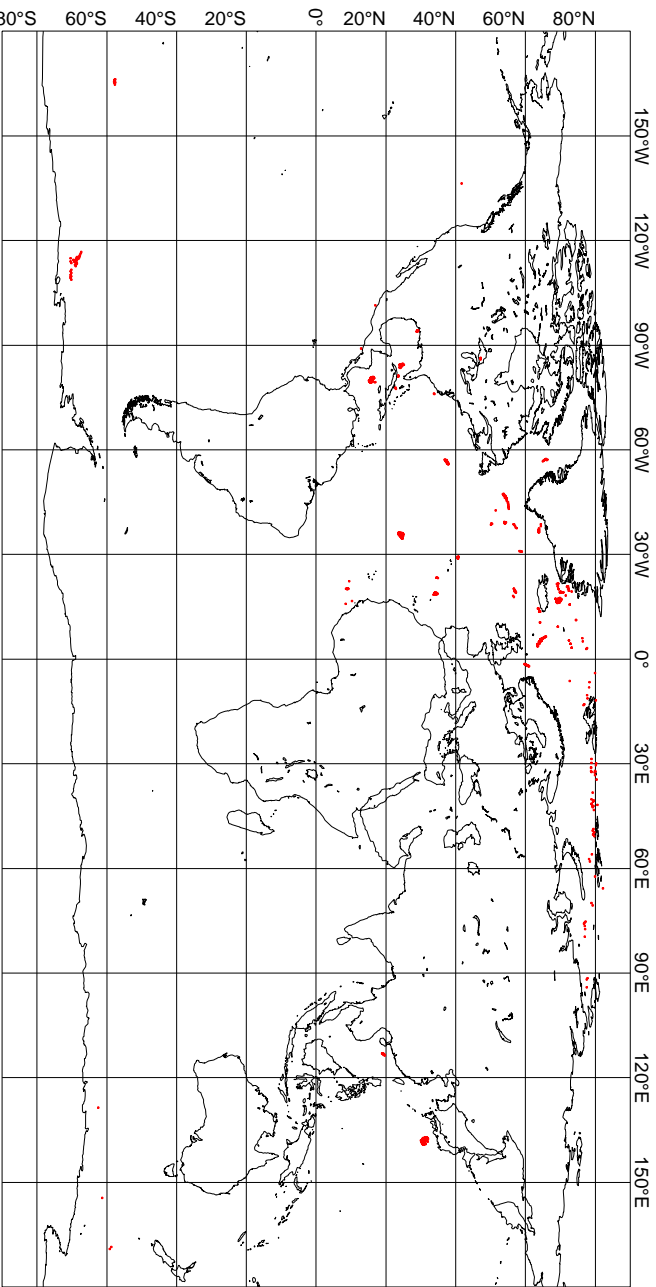


Figure 11

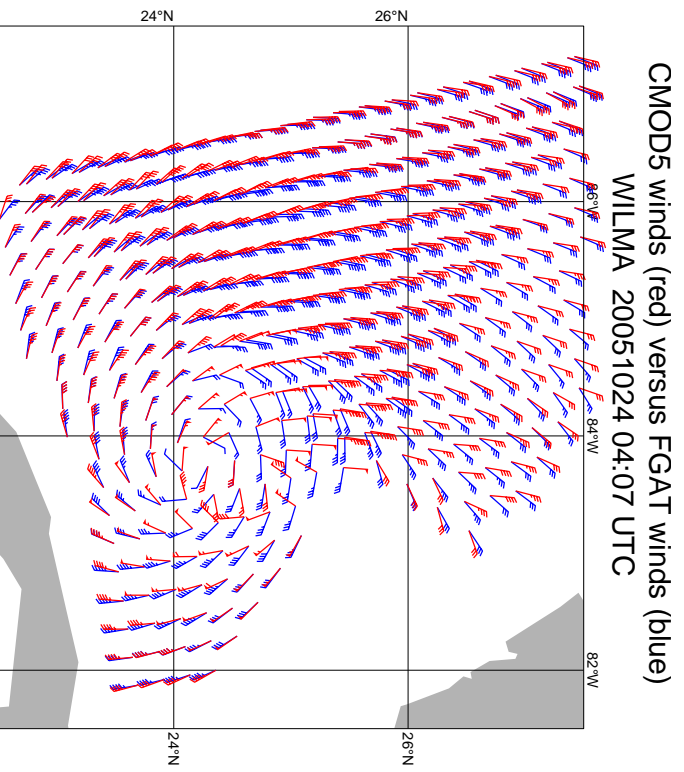
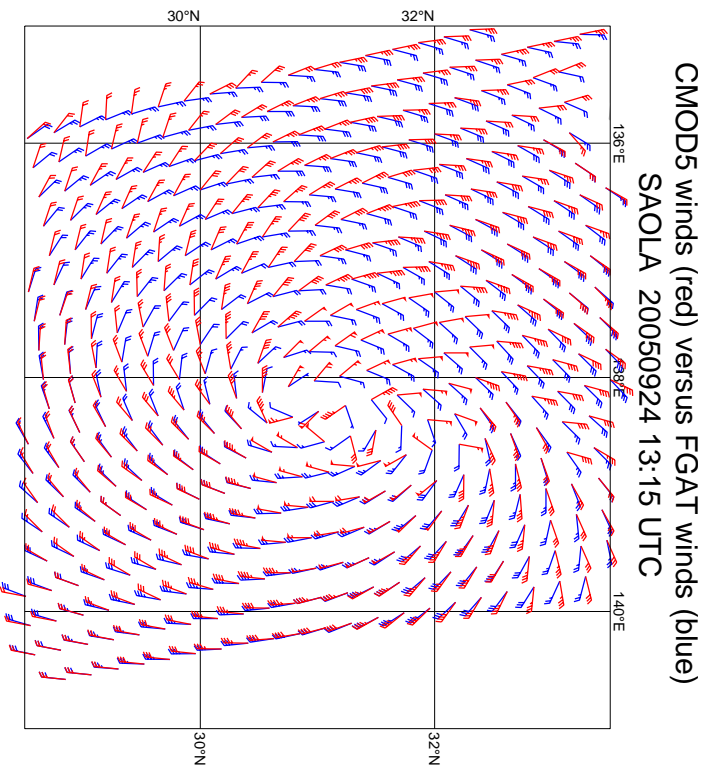
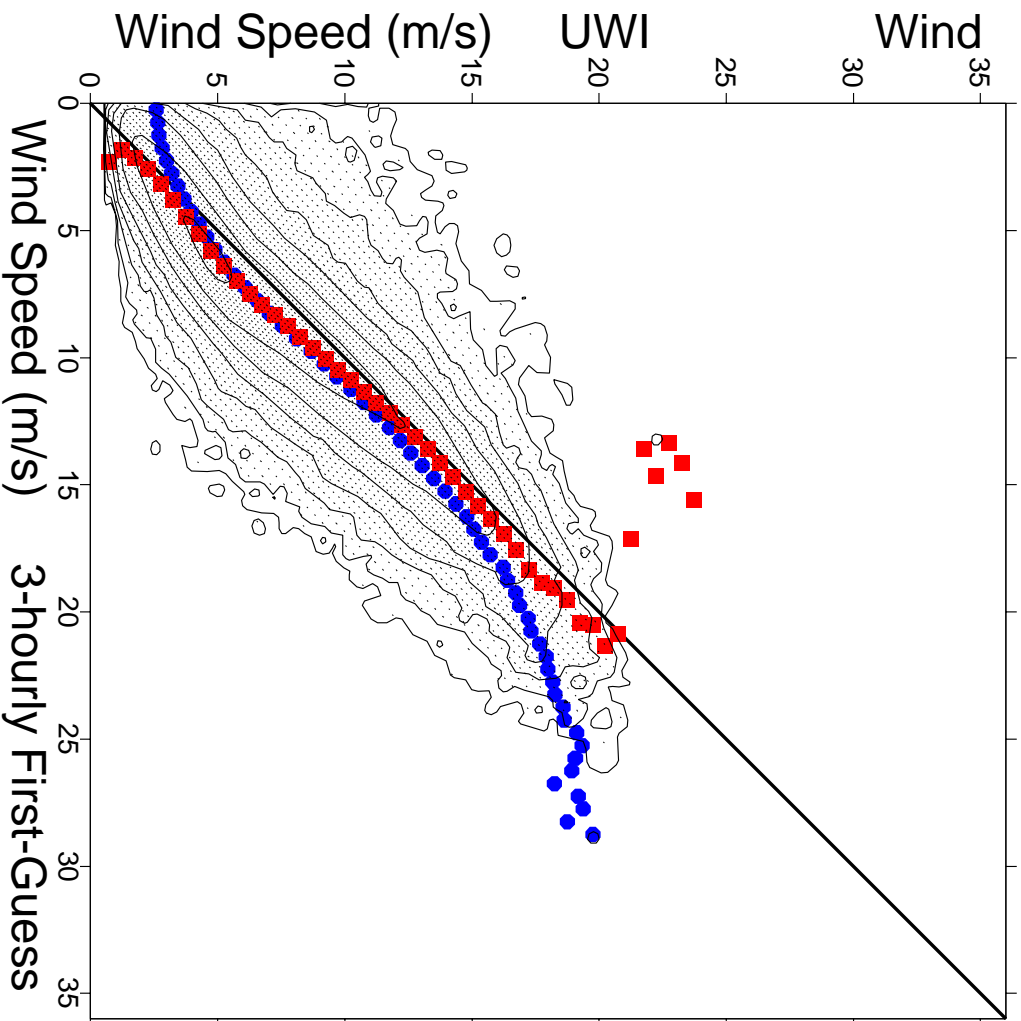


Figure 12



ECMWF 3-hourly First-Guess winds versus UWI winds  
 from 2005092000 to 2005102418  
 = 1031939, db contour levels, 5 db step, 1st level at 5.1 db  
 $m(y-x) = -0.82$   $sd(y-x) = 1.52$   $sd_x = 3.88$   $sd_y = 3.65$   $pcxy = 0.959$

Figure 13

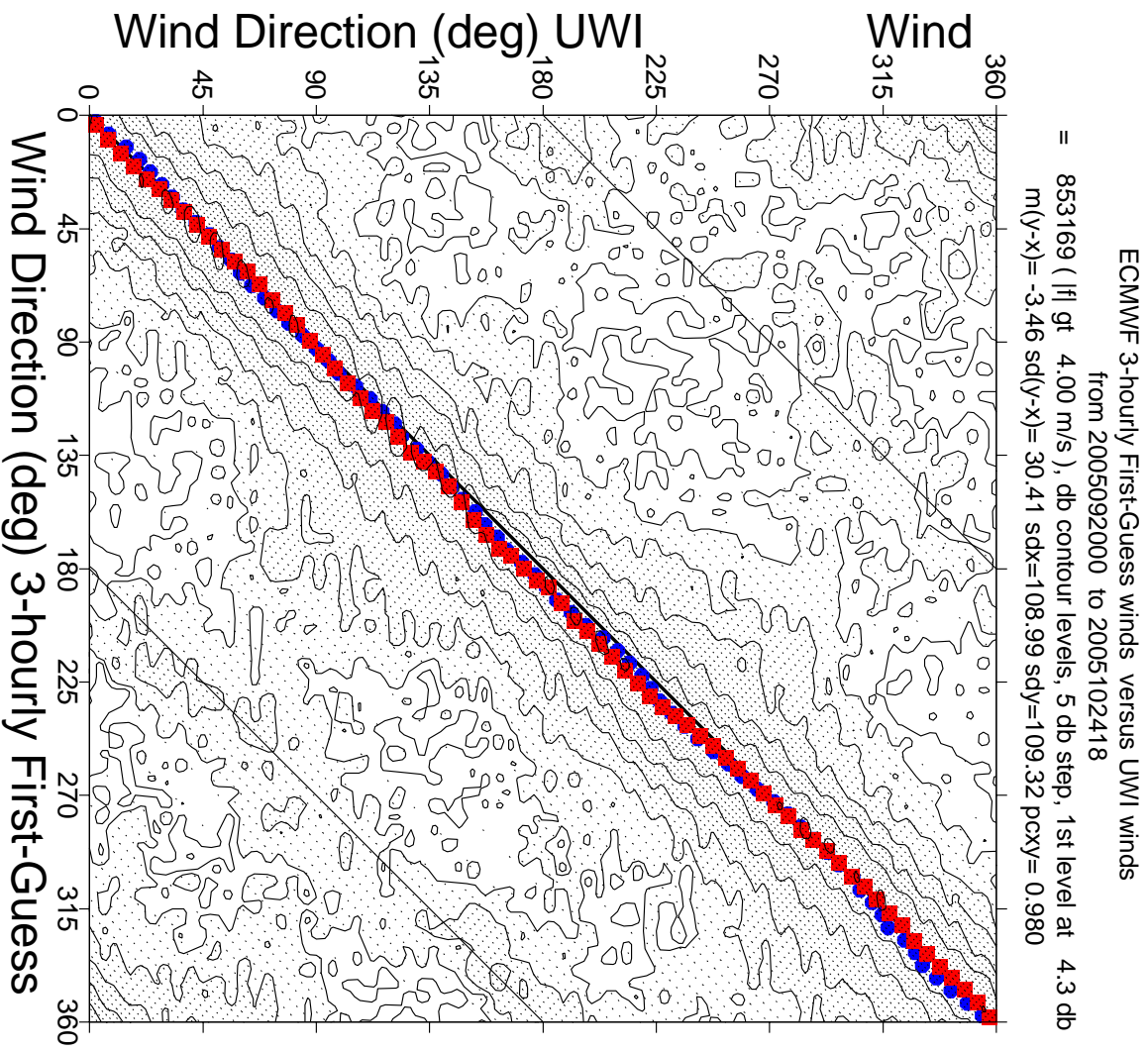


Figure 14

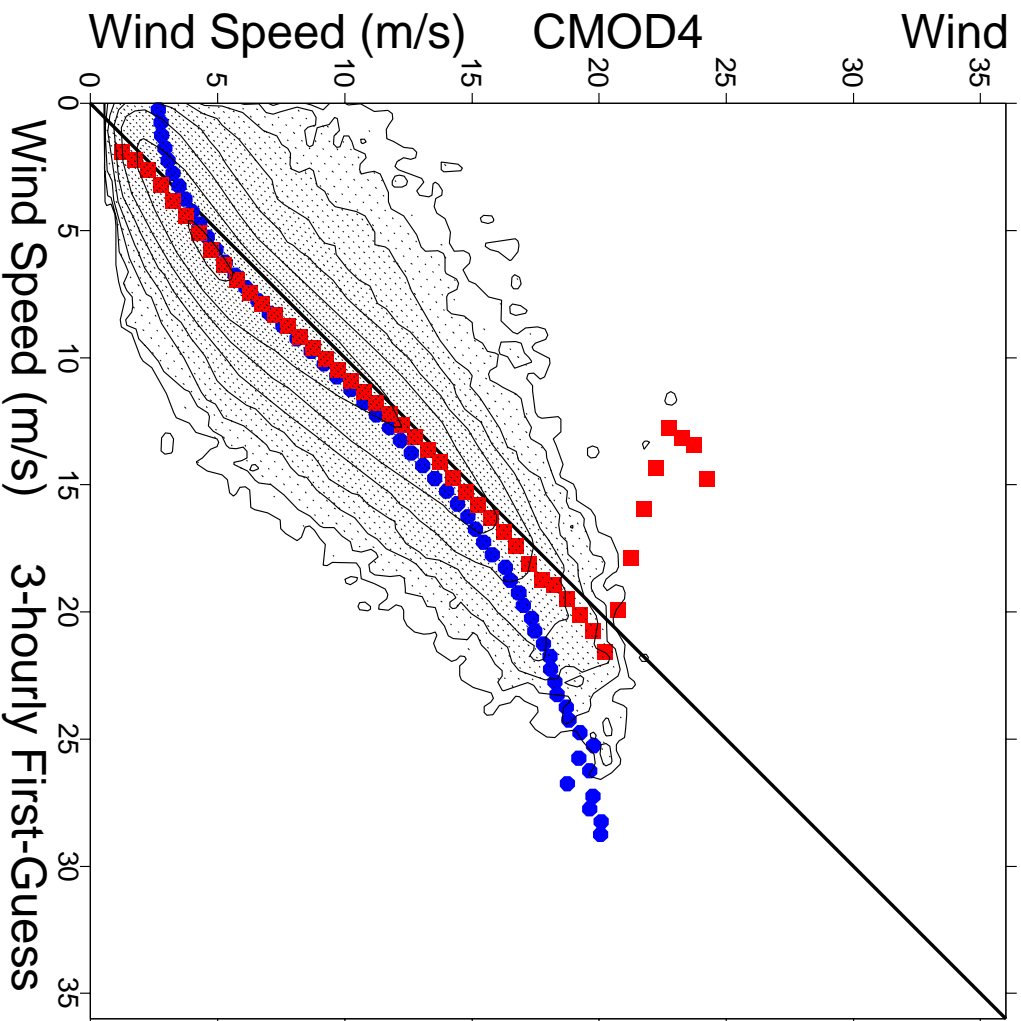


Figure 15

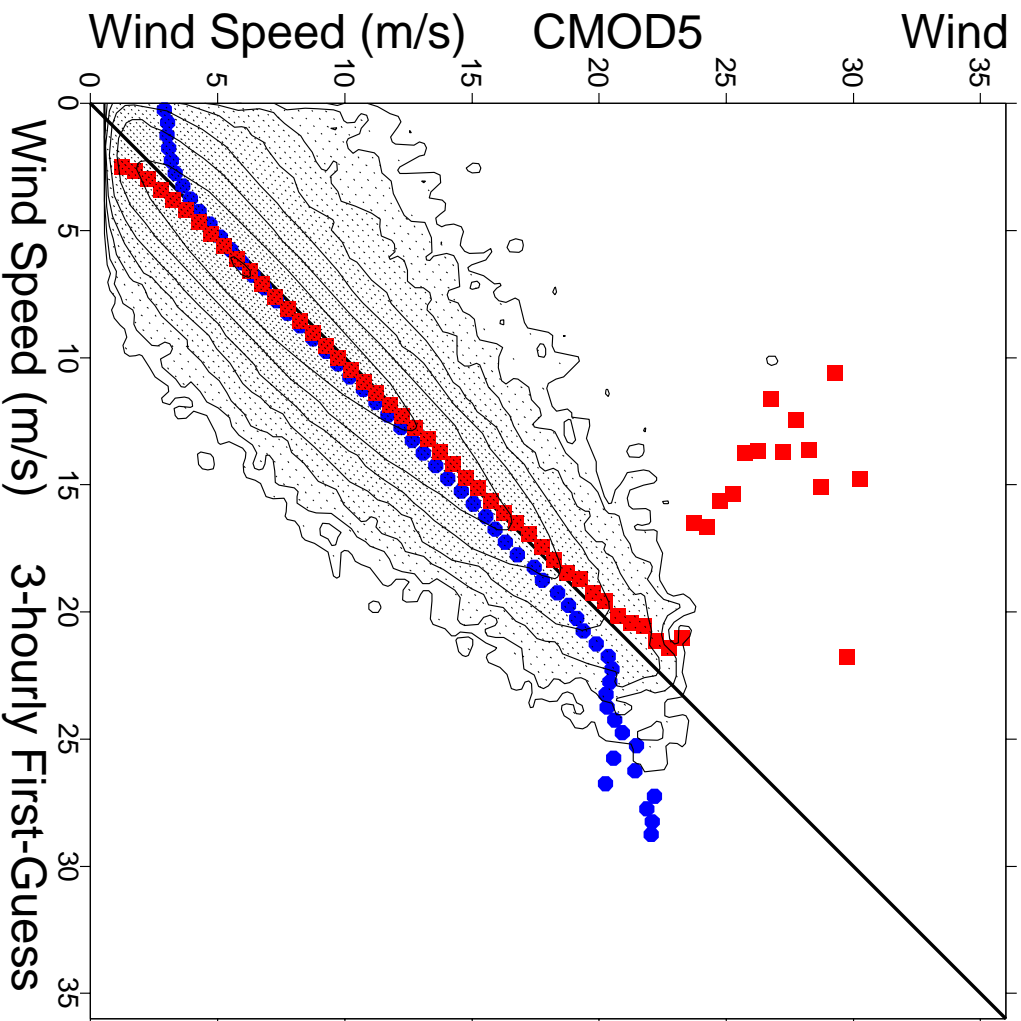
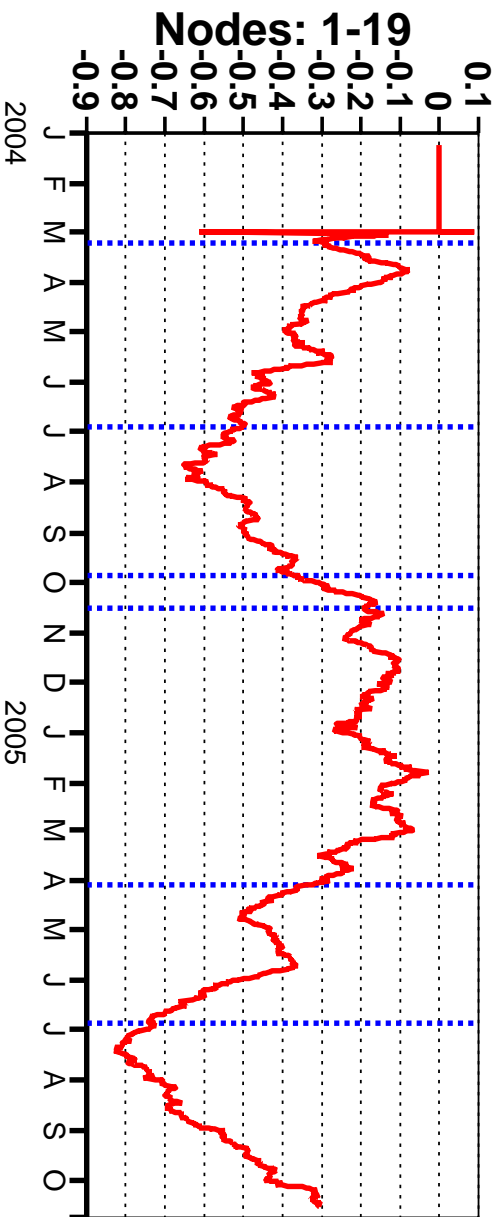


Figure 16

# ERS-2 (CMOD5)



# QuikSCAT (QSCAT-1)

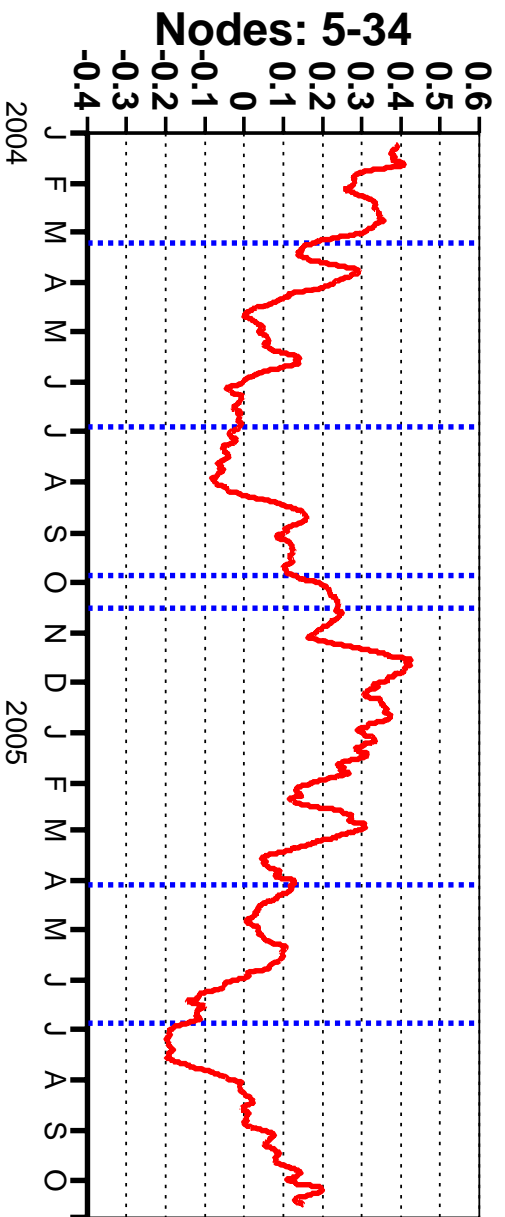


Figure 17